

RECENT ACHIEVEMENTS IN DESIGNING ZEOLITE CATALYSTS

MARIYA SHAMZHY

Department of Physical and Macromolecular Chemistry, Faculty of Science, Charles University, Hlavova 8, 128 43 Prague 2, Czech Republic
mariya.shamzhy@natur.cuni.cz

Received 27.2.23, accepted 12.6.23.

Zeolites are porous crystalline solid acid catalysts that are widely used in the petrochemical industry and have high potential for new catalytic applications. This paper provides an overview on recent progress in the design of zeolite catalysts *via* chemical and structural modification of germanosilicates combined with IR spectroscopic studies to address the synthesis-structure-performance relationships in the new catalytic materials.

Keywords: Zeolite catalysts, acid sites, germanosilicates, synthesis-structure-function relationships, *in situ* IR spectroscopy

Contents

1. Introduction
2. Zeolite catalyst design by modification of germanosilicates
 - 2.1. Tuning of the chemical composition with maintenance of zeolite structure
 - 2.2. Tuning of the chemical composition and zeolite structure
 - 2.3. Ge recycling
3. IR spectroscopic *in situ* studies of zeolite catalysts
4. Conclusions and outlook

1. Introduction

The phenomenon of catalysis is known as an increase in the rate of a chemical reaction in the presence of a substance called the catalyst. An important feature that distinguishes the catalyst from the reactant is that a catalyst is not consumed or changed as the reaction is completed. A particularly important class of industrially relevant catalysts are zeolites, the crystalline microporous solid acids. From a chemical point of view, zeolites are elementosilicates, the frameworks of which are made of corner-sharing tetrahedra TO_4 ($T = Si, Al, Ti$) (Fig. 1, left)¹. Elements with typical oxidation state +3, such as Al, impose a negative framework charge and give rise to Brønsted acidity, when compensated by a proton (Fig. 1, right).

Brønsted acid sites (BAS) enable Al-substituted zeolites to catalyze various chemical reactions, such as cracking, isomerization, alkylation or acylation used in petrochemical industry. In turn, the presence of coordinatively unsaturated atoms of four-valent elements, such as Ti or

Sn, in a zeolite framework results in formation of Lewis acid sites (LAS), which are active in various reactions for the catalytic valorization of biomass-derived compounds (e.g., glucose-to-fructose isomerization, Baeyer-Villiger oxidation of ketones to esters, or Meerwein-Ponndorf-Verley (MPV) reduction of carbonyl compounds to the respective alcohols)³.

Zeolites are very stable solids that resist the conditions which challenge many other materials⁴. Specifically, aluminosilicate zeolites are stable up to 600–800 °C, they do not dissolve in water or organic solvents and do not oxidize in the air. But the most interesting characteristic of zeolites is their open porous structure. Each pore in a zeolite accommodates the molecules to be transformed. Countless number of such pores act like millions of nano-reactors where chemical reactions take place on acid sites.



Mariya Shamzhy graduated from Lomonosov University and received her Ph.D. degree at the Ukrainian Academy of Sciences. She spent 1 year as a postdoctoral fellow at J. Heyrovsky Institute of Physical Chemistry under the supervision of Prof. J. Čejka. Today, Dr. Shamzhy works as an Associate Professor at the Faculty of Science at the Charles University, where she leads the research team focusing on the design of new type of single-site zeolite catalysts. For her research on porous materials, Mariya Shamzhy has received “Neuron Prize 2022 for Promising Scientists in chemistry”.

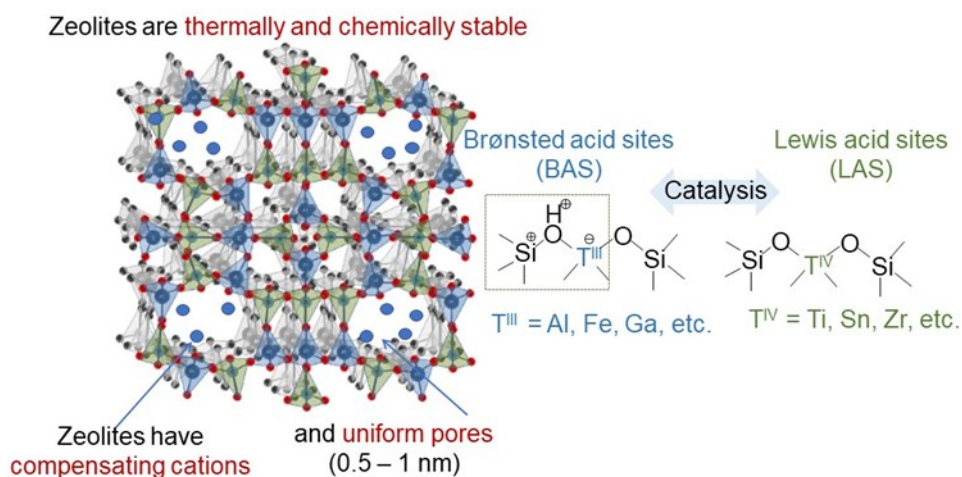


Fig. 1. A zeolite framework (left). Brønsted and Lewis acid sites in zeolites (right). Adapted from²

Since the pores in a particular zeolite have a fixed size in the range of kinetic diameters of small organic molecules (Fig. 2), an optimized catalyst can selectively interact only with the molecules of appropriate size, selectively producing the demanded product⁵. There are three types of so-called shape selectivity of a zeolite. *Reactant shape selectivity* excludes from the catalytic cycle the molecules of reactant that are larger than the pores of a zeolite. *Product shape selectivity* decreases the diffusion of large products, which were formed in zeolite pore system. *Transition-state shape selectivity* restricts the formation of intermediates that are larger than zeolite pores.

There exist (i) natural zeolites, (ii) synthetic analogues of natural zeolites, and (iii) synthetic zeolites with no natural analogues, together more than 250 structural types⁷. Each of those structural types is represented by a three-letter code assigned by the Structure Commission

of the International Zeolite Association (SC-IZA)⁷. *Natural zeolites* are mined in various parts of the world and are used in environmental protection, agriculture, and construction (Fig. 3, top). The largest deposits are located in China, South Korea, New Zealand, United States, and Slovakia⁸. In nature, zeolites crystallized mostly as aluminosilicates due to the deposition of volcanic ash in ancient alkaline lakes and the transformations that occur under hydrothermal conditions. *Synthetic zeolites* used for industrial applications in adsorption and catalysis are being produced by mimicking the conditions under which natural zeolites were formed. The hydrothermal crystallization of a zeolite in a chemical laboratory is completed in several days compared to millions of years in nature. For hydrothermal crystallization of synthetic zeolites, various sources of framework-building elements (e.g., silica, aluminum chloride, titanium chloride, etc.), alkaline metal

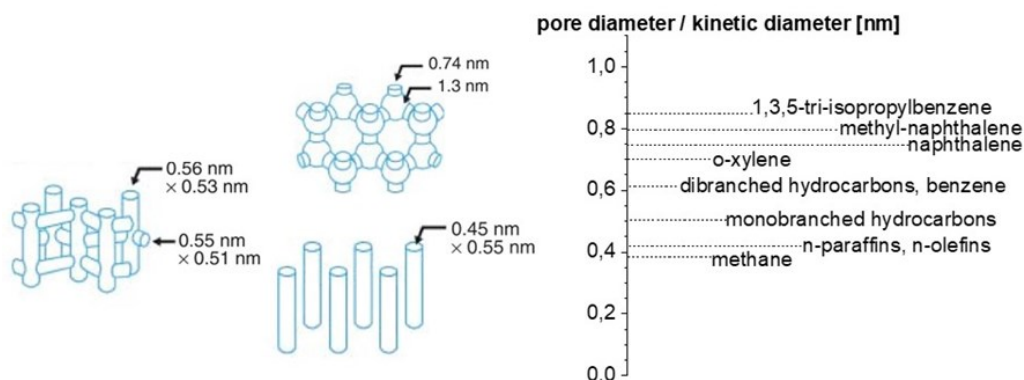


Fig. 2. The kinetic diameters of selected organic molecules compared to the pore sizes of zeolites. Adapted from⁶

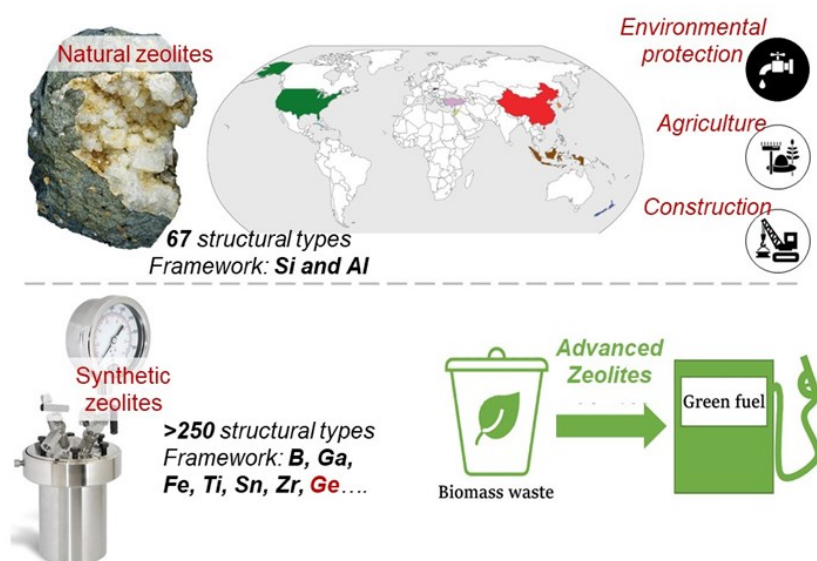


Fig. 3. Chemical and structural variability of natural and synthetic zeolites. Adapted from¹¹

hydroxides or organic bases (e.g., tetraalkylammonium hydroxides) and water are mixed and subjected to the chemical reaction at high temperature (100–200 °C) and autogenous pressures⁹. In this way, synthetic chemists could make new materials with structural and compositional properties far more diverse than those of natural minerals (Fig. 3, bottom)^{3,10}. Nowadays, the tailoring of the chemical composition of zeolite catalysts is considered prospective to expand the application scope of these efficient catalysts to biomass-derived feedstock.

The aim of this work is to familiarize readers with recent achievements in the design of new zeolite catalysts with a special focus on zeolites discovered in the Czech Republic. Section 2 describes synthetic approaches to tuning the nature of active acid sites in synthetic zeolites containing germanium atoms. The application of *in situ* infra-red spectroscopy (IR spectroscopy) for understanding the relationships between the synthesis parameters, physicochemical properties and catalytic performance of the designed zeolite catalysts are discussed in Section 3. Finally, the outlook for future activities in zeolite catalyst research is proposed.

2. Zeolite catalyst design by modification of germanosilicates

Al and Si are the most abundant framework-building elements in natural zeolites, whereas the framework charge is compensated for by alkaline and alkaline earth

metal cations. In contrast, synthetic materials have much more diverse chemical compositions, because various metals can be incorporated into zeolite frameworks using different commercially available inorganic compounds, whereas the framework charge can be compensated for by organic cations¹². A particularly interesting family of synthetic zeolites consists of germanosilicates. According to its chemical properties (e.g., electronegativity, coordination number), germanium is the closest element to silicon. Therefore, germanium can be isomorphously substituted into various zeolite structures, previously known as silicates or aluminosilicates^{13,14}. On the other hand, germanium differs significantly from silicon in some properties. For example, the Si–O bond length for four-coordinated silicon is typically in the range 0.160–0.163 nm, while the Ge–O bond length is in the range 0.170–0.180 nm (ref.¹⁵). The T–O–T angles in germanates are much smaller (117–145°) than in silicates (135–180°)¹⁵. Thanks to the mentioned properties, germanium facilitates the formation of previously unknown zeolite structures that contain small structural units such as cubes (D4R) or triangular prisms (D3R)^{16–21}. Some of these structures have exceptionally large pores (0.85–1.2 nm) that are essential for shape-selective chemical reactions of bulky molecules²².

Germanosilicate zeolites, however, contain very weak acid centers that do not catalyze most reactions of industrial importance, such as Friedel–Crafts acylation of aromatic hydrocarbons and MPV reduction of ketones to alcohols. In addition, the presence of germanium in the structure reduces the hydrolytic stability of the zeolite due

to the high lability of the Ge-O-Si and Ge-O-Ge bonds in the presence of water. To overcome the mentioned shortcomings of germanosilicate zeolites, Ge-for-metal substitution was proposed and optimized for tailoring various catalytically active centers in these structurally interesting zeolites. This section will provide several examples of exploiting hydrolytic instability of Ge-O-Si bonds to tune the acid properties of germanosilicate zeolites which can be implemented either with the preservation of the original zeolite structure (Section 2.1) or combined with the structural transformation of the original structure into a new zeolite (Section 2.2). The recycling of expensive Ge is discussed in the context of cost-effective production of new catalytic materials in Section 2.3.

2.1. Tuning of the chemical composition with maintenance of zeolite structure

Germanosilicate zeolites were prepared with varying Si/Ge molar ratio, using germanium oxide as the germanium source and with a suitable organic agent to stabilize the specific zeolite structure (Table I). The structure of all germanosilicates under study can notionally be viewed as crystalline silica layers of different thickness (shown in Table I in black) covalently connected *via* Ge-enriched cubic D4R units (shown in Table I in red). The molar ratio of the framework atoms (Si/Ge) in a zeolite determines the number of Ge-O-Si and Ge-O-Ge links and thus affects the hydrolytic stability of germanosilicates. Zeolites with less than or equal to two hydrolytically unstable interlayer bonds in the D4R units (e.g., zeolite assigned by SC-IZA as CTH with Si/Ge > 15) retain structure in aqueous media. On the other hand, zeolites with 4 hydrolytically unstable interlayer bonds (e.g., CTH with Si/Ge < 7) decompose in aqueous media (Table I).

X-ray diffraction (XRD) studies revealed that in acidic aqueous solution (pH 0.5–2.0) germanosilicates with high content of Ge (with typical Si/Ge ratios in the range

of 1 to 6.4, depending on the structure of the zeolite) can collapse (Fig. 4) or undergo the so-called framework disassembly by removal of Ge atoms, giving highly ordered materials composed of crystalline and relatively independent layers^{23–30}.

This provides an opportunity to manipulate the interlayer unit organization towards zeolite catalysts with new structures (*vide infra*). However, the same zeolites maintain their structural characteristics, if acidic treatment is carried out in the presence of Al³⁺ cations (Fig. 4)^{31–33}. The obtained result was formally explained (see Fig. 5) by rapid healing of defects (see system A in Fig. 5) formed upon hydrolysis of Ge-O-Si bonds in the parent germanosilicate (see system B in Fig. 5) by Al with a formation of Al-O-Si bonds (see system C in Fig. 5).

To understand the observed phenomenon in more detail, a time-resolved *ex situ* characterization of hydrolysis intermediates was performed. For that, the evolution of UOV zeolite with Si/Ge = 3.1 was followed with time of hydrolysis³³. According to the results of the chemical analysis, most Ge left the framework after 5 min, while the Al concentration reached maximum after several days. XRD analysis showed that degermanation led to a partial deconstruction of the framework as the interlayer distance decreased. In turn, incorporation of aluminum into the framework completely restored the zeolite structure as interlayer (100) diffraction line returned to the original position. The obtained results reveal that the insertion of Al into germanosilicate zeolite framework proceeds *via* fast removal of Ge from the structure, followed by slow incorporation of aluminum.

The incorporation of Al atoms into the framework positions of germanosilicate zeolites upon discussed post-synthesis treatments was confirmed by solid state ²⁷Al MAS NMR, while the formation of strong acid sites was verified by *in situ* IR spectroscopy after adsorption of pyridine, used as a probe molecule (*vide infra*).

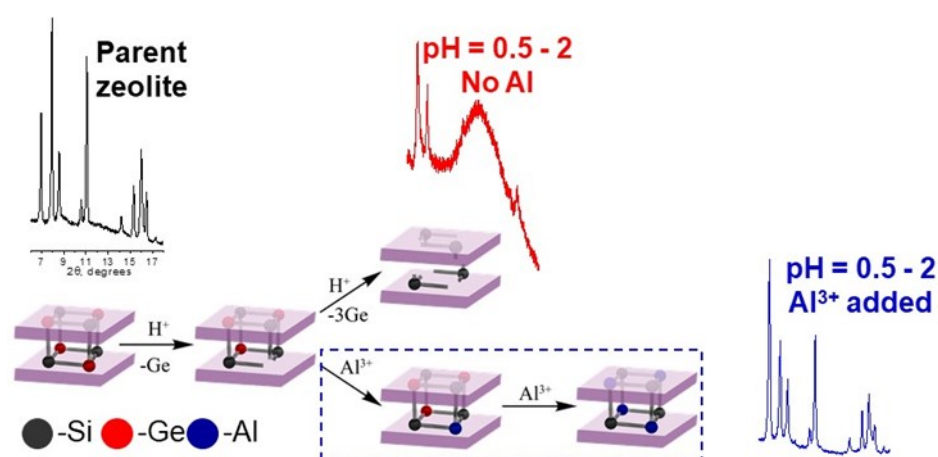
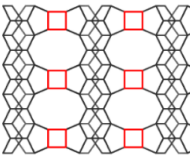
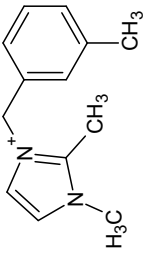
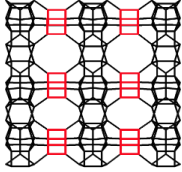
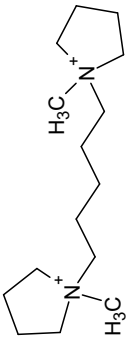
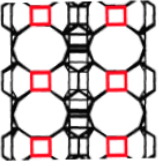
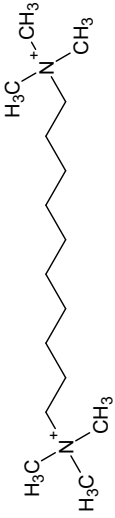
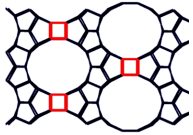
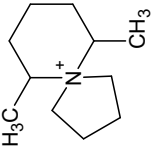


Fig. 4. XRD analysis of germanosilicate behavior in Al-containing and Al-free acidic medium

Table I
The germanosilicate zeolites under study

Three-letter code of a zeolite assigned by SC-IZA	Framework	Organic compound used for the synthesis	Synthesized materials	Si/Ge molar ratio in the framework of	
				Hydrolytically unstable zeolite	Hydrolytically stable zeolite
CTH			3.8–6.4	<7	>15
IWW			1.0–5.0	<6	>13
UOV			1.3–3.3	<6	>13
UTL			3.7–6.0	<8	>18

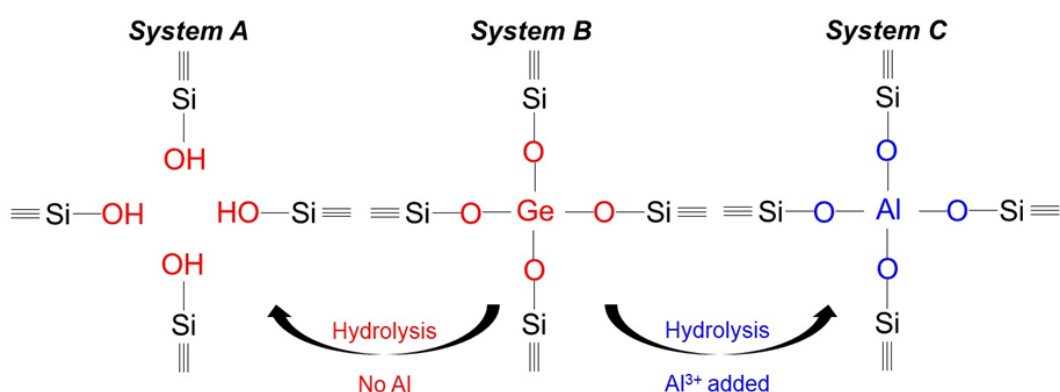


Fig. 5. Local structure of systems formed during targeted manipulation of the interlayer unit organization in germanosilicate zeolites towards zeolite catalysts with new structures (*vide infra*). A – system of silanol groups formed by hydrolysis of Ge-O-Si bonds in the absence of Al; B – system of Ge-O-Si bonds in the parent germanosilicate; C – system of Al-O-Si bonds formed by hydrolysis of Ge-O-Si bonds in the presence of Al

In addition to Al, other three-valent elements such as B and Ga were incorporated into germanosilicate zeolites^{34–37}. The prepared catalytic materials were active in the Friedel-Crafts acylation of *p*-xylene (Fig. 6, left) that selectively produces 2,5-dimethylbenzophenone, which is widely used as a UV light stabilizer in plastics, cosmetics, and films^{38,39}.

Based on the results of IR spectroscopy of adsorbed pyridine, the samples contained a similar number of acid sites but a different fraction of strong acid centers, which increased in the following sequence: B < Ga < Al. The

weak acid sites of the parent germanosilicate zeolite and zeolite substituted with B showed low activity in the reaction. Al-acid sites were active, but rapidly deactivated because of the strong adsorption of 2,5-dimethylbenzophenone⁴⁰. The highest yield was achieved on Ga-containing zeolite with moderate acid strength because such active sites enable sufficient activation of the reagent and easy desorption of the product.

Substitution of Ge for Zr resulted in the active catalyst for the MPV reduction of ketones to alcohols (Fig. 6, right). Similarly to the Friedel-Crafts acylation, the parent

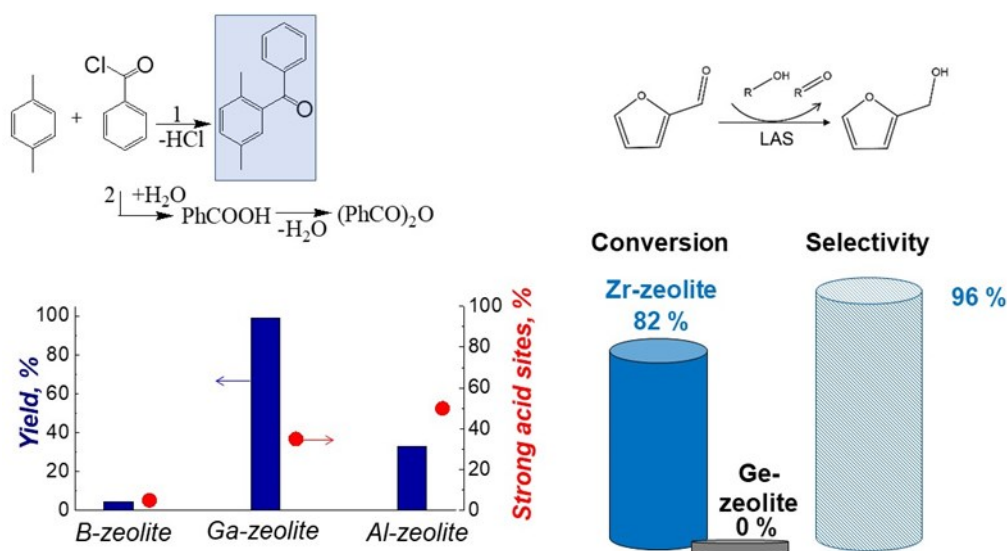


Fig. 6. Catalytic performance of three-valent element-substituted zeolites in the benzoylation of *p*-xylene (left) and Zr-substituted zeolite in the MPV reduction of furfural (right). Red dots show the relative concentration of strong acid sites determined using thermodesorption of pyridine monitored by IR spectroscopy

germanosilicate was inactive in MPV reduction, but Ge-for-Zr substitution allowed us to achieve high conversion (82%) and selectivity (96%) values.

Thus, post-synthesis modification of the chemical composition while maintaining structure integrity of germanosilicate zeolites allows to optimize the properties of these structurally interesting materials for acid-catalyzed reactions that require active centers of various types. This method made it possible to synthesize zeolite catalysts with such structural and chemical properties that have been difficult or even impossible to achieve using standard hydrothermal synthesis protocols.

2.2. Tuning of the chemical composition and zeolite structure

In contrast to the Ge-poor zeolites (with less than or equal to two hydrolytically unstable interlayer bonds per D4R unit, Table I), Ge-rich zeolites (with 4 or more hydrolytically unstable interlayer bonds per D4R unit, Table I) may completely disassemble into crystalline layers in pure water. This means that hydrolysis breaks all interlayer bonds in a short time (~5 min), which is detected by a significant decrease in the interlayer distance by XRD analysis (Fig. 6, left). As water participates in the breaking of the interlayer bonds⁴¹, we anticipated that a decrease in the water concentration would decelerate the deconstruction process. Therefore the behavior of hydrolytically unstable UTL zeolite with Si/Ge ratio of 4.5 was studied in mixed water-methanol systems⁴². Unlike aqueous medi-

um, the size of interlayer units in UTL zeolite gradually decreased over time in 60% methanol (Fig. 6, left).

To incorporate catalytically active centers, Al was added to the system, and the picture changed significantly (Fig. 7, right). A remarkable increase in the lifetime of the parent zeolite was observed. After a certain time, the D4R units in UTL reduced in size, forming zeolite IPC-2 with S4R interlayer connections. Surprisingly, with prolongation of the treatment up to 60 days, the original UTL framework was restored, as confirmed by the results of XRD analysis (Fig. 7, right) and TEM. The recovered UTL (Si/Ge = 9; Si/Al = 24) had much higher concentration of Brønsted and Lewis acid sites ([BAS] = 0.30 mmol g⁻¹, [LAS] = 0.20 mmol g⁻¹) in comparison to the hydrothermally synthesized UTL (0.05 and 0.04 mmol g⁻¹), which is a benefit of the proposed synthetic method.

By varying the conditions (e.g., pH, time) of UTL germanosilicate hydrolysis, we have prepared a series of Al- (ref.⁴³) and Ti-substituted⁴⁴ zeolites with the same layer structure but with different interlayer connectivities (e.g., D4R, S4R, -O-) and different micropore sizes. Catalytic activity is an important property of all zeolites prepared in this way. For example, Al-substituted UTL-derived zeolites were tested in the model reaction of alcohol tetrahydropyranlation (Fig. 8, left)⁴³. We varied the size of reagents, such as ethanol, 1-hexanol, and 1-decanol. The smallest ethanol molecules showed similar conversions in all the catalysts. On the contrary, the conversions of bulky alcohols dramatically decreased with the micropore size.

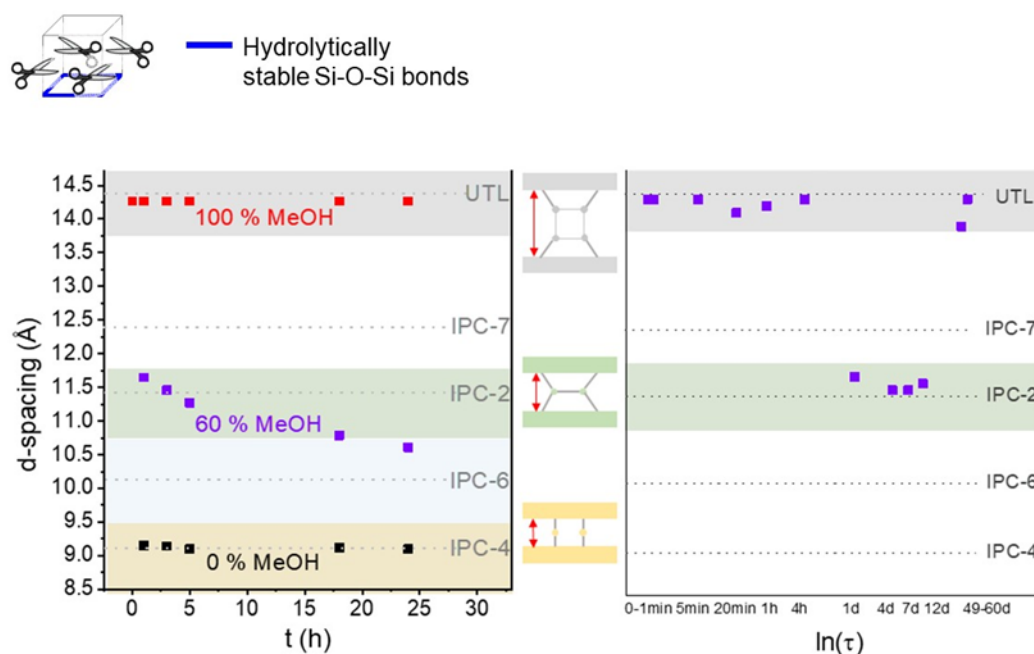


Fig. 7. Interlayer d-spacing in UTL germanosilicate in Al-free (left) and Al-containing (right) water/methanol medium

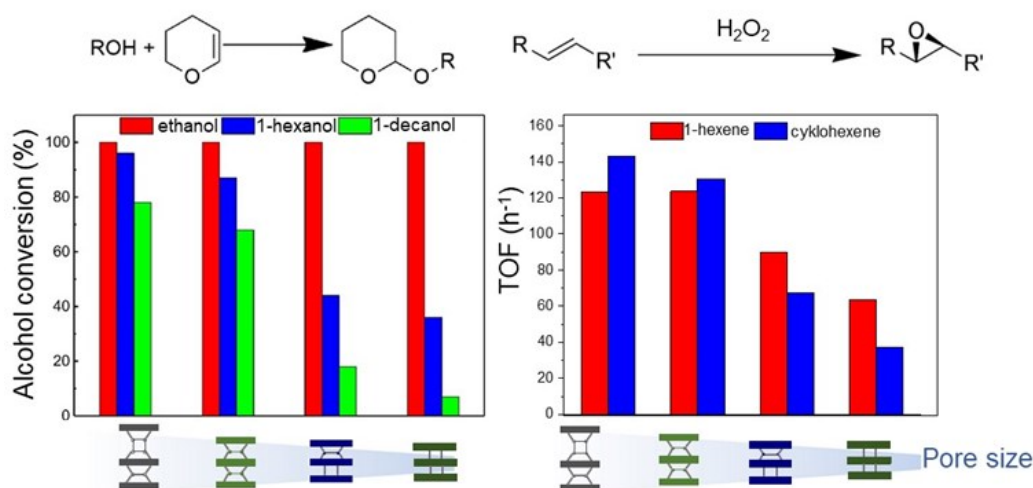


Fig. 8. Conversion (left) and activity (right) of Al- and Ti-substituted UTL-derived zeolite catalysts with different interlayer connectivities

Similarly, in the epoxidation of bulky cyclohexene over Ti-substituted zeolites, the highest activity was achieved over the catalyst with the largest pores (Fig. 8, right)⁴⁴. Because these findings match the results expected from the predictive kinetic analysis, the zeolites prepared by tailoring the chemical composition and structure of UTL germanosilicate were proposed as model catalysts to assess the activity-pore size relationships.

2.3. Ge recycling

Due to the rare abundance and high price of Ge used for the preparation of new catalytic materials, we have focused on the possibility of Ge recovery and recycling in further synthesis and came up with the method that allows

one to recover more than 90% Ge from the parent zeolite and reuse it for the preparation of new germanosilicate materials (Fig. 9)⁴⁵.

The approach is based on the repetitive treatment of the initial germanosilicate with water, followed by separation of the parent zeolite from mother liquor by filtration using filter paper Fischer Scientific of 601 grade (the pore size in the range 5–13 μm) or microfiltration using membrane filter paper MF-Millipore™ (the pore size of 0.025 μm). After evaporation of an excess of water used for hydrolysis, GeO_2 is recovered.

It was found that the method for GeO_2 separation determines the phase selectivity of zeolite formation upon Ge recycling. If filtration is used, the recovered GeO_2 contains microcrystals of the parent zeolite with a size of

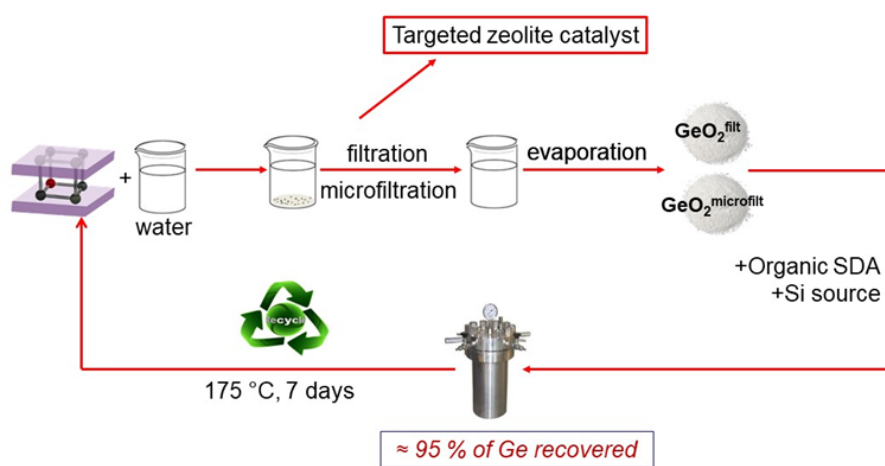


Fig. 9. The method proposed for recycling of Ge for the preparation of zeolites

0.5 μm . These remaining particles serve as seeds, which facilitate the formation of the parent zeolite independently of the synthesis conditions. Such a source of germanium may be prospective for the organic-free preparation of desired germanosilicates. In contrast to filtration, microfiltration allowed careful removal of the zeolite seeds and enabled the recovery of germanium oxide, which can be used for the synthesis of different zeolite structures.

3. IR spectroscopic *in situ* studies of zeolite catalysts

The design of zeolite catalysts for specific applications is important, but practically impossible without understanding the surface chemistry of the prepared materials. IR spectroscopy is a useful method suitable for studying the surface properties of various catalysts⁴⁶. *In situ* IR spectroscopy makes it possible to study the catalyst surface under various conditions and in diverse media. For example, by studying the processing of a zeolite at varying temperatures, the optimal activation conditions for complete dehydration of a catalyst can be determined. A detailed study of the strength, location, nature, and concentration of acid centers in zeolites is usually realized by adsorption (or, pertinently, desorption) of probe molecules monitored spectroscopically. Pyridine is among the most accepted basic probe molecules for this purpose^{47,48}. Specific bands, arising from the interaction of pyridine with acid centers of various nature in the region of 1700–1400 cm^{-1} , allow one to distinguish Lewis (1445 and 1611 cm^{-1})

and Brønsted (1545 and 1638 cm^{-1} , Fig. 10) acid sites, while the intensity of respective bands is directly related to the concentration of these acid centers.

An IR spectroscopic *in situ* study allowed us to understand the active sites responsible for glycerol ketalization to solketal over germanosilicate zeolite IWW (Fig. 10)⁴⁹. An interesting finding was an increasing conversion of glycerol over IWW germanosilicate with a decreasing activation temperature. Using thermodesorption of pyridine, it was found that decreasing the activation temperature resulted in an increase in the concentration of the BAS at the expense of the LAS. Noticeably, the adsorption of water on the activated zeolite changed the distribution of acid sites in the IWW zeolite in a similar way (Fig. 10). The obtained results indicate the possibility of the formation of weak Brønsted acid centers upon the polarization of water molecules coordinated with LAS in IWW zeolites (Fig. 10, right). The catalytic results reveal a higher activity of thus formed Brønsted acid sites in the ketalization reaction if one compares it with the Lewis acid centers.

In situ IR spectroscopy is also informative for the study of zeolite catalysts, not related to germanosilicates. The next example shows how the IR spectroscopic *in situ* study helped to understand the difference in catalytic behavior of two catalysts in transformation of biomass-derived furfural⁵⁰. The first catalyst produced exclusively furfuryl alcohol (shown in Fig. 11 in blue) and the second catalyst yielded methylfuran (shown in red).

To understand this selectivity, IR spectroscopic *in situ* study was focused on the interaction of catalyst sur-

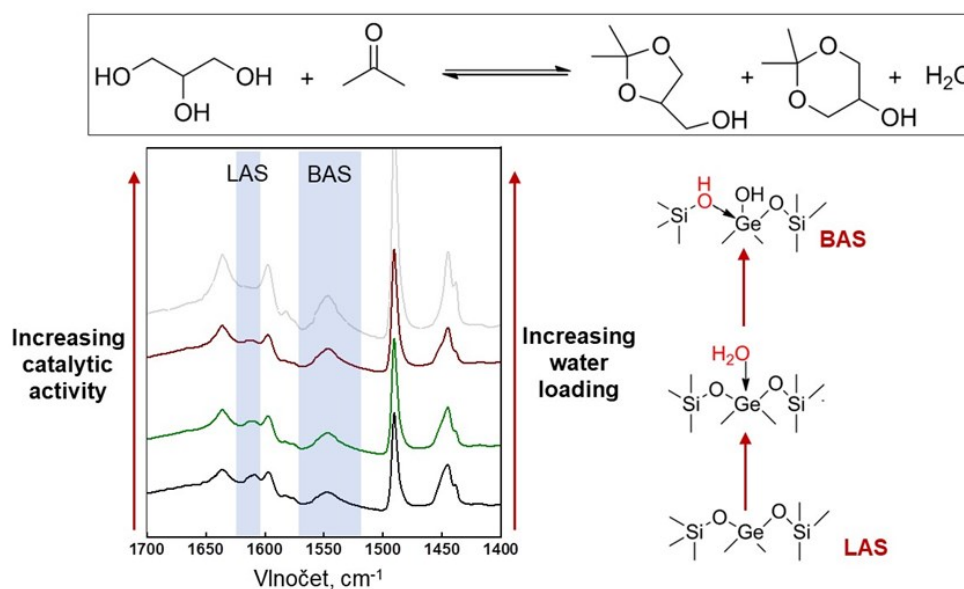


Fig. 10. IR spectroscopic *in situ* study of active sites responsible for ketalization of glycerol to solketal (top) on germanosilicate zeolite IWW. IR spectra of pyridine adsorbed in IWW zeolite activated at 450 °C and subsequently loaded with water (left). Proposed mechanism of the water-induced formation of BAS in IWW germanosilicate (right)

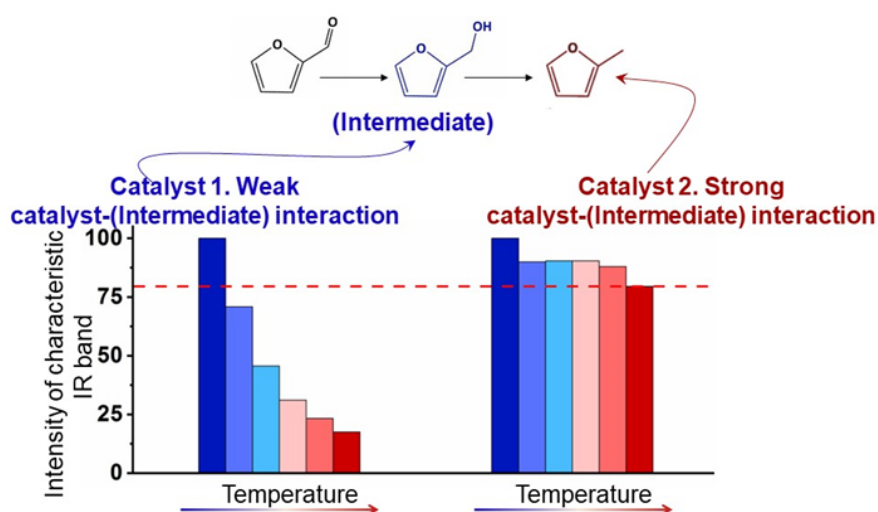


Fig. 11. Transformation of furfural over Rh catalyst supported on Na-form (Catalyst 1) and H-form (Catalyst 2) of zeolite BEA along with the results on thermodesorption of intermediate compound monitored by IR spectroscopy

face with the furfuryl alcohol considered intermediate on the way to methylfuran. Upon heating, intermediate molecules rapidly leave the surface of the first catalyst (Rh catalyst supported on *sodium* form of zeolite BEA), indicating weak interaction with the solid, which may account for the termination of the reaction as soon as furfuryl alcohol is formed. On the contrary, the special functionality of the second catalyst (Rh catalyst supported on *proton* form of zeolite BEA) ensures a strong interaction with the intermediate, which may condition its transformation into methylfuran. An understanding of the structure-function relationship using *in situ* spectroscopic methods is an unavoidable step in the design of efficient catalysts for practical applications.

4. Conclusions and outlook

The presented examples on recent achievements in designing zeolite catalysts combine

- synthetic methods developed for zeolites with unusual structures/compositions *via* post-synthesis modification of germanosilicates and
- IR spectroscopic *in situ* studies of catalyst surface chemistry for understanding catalytic transformation at the molecular level.

Despite these recent advances, our traditional synthetic methods and experimental approaches seem to have reached their limits when considering further development. For example, to find the optimal zeolite catalyst for a particular reaction, we usually go into the toolbox of available zeolites, test them, try to find an explanation for their specific behavior, and then repeat the cycle. However currently available synthetic zeolites contain a variety of acid sites located in different crystallographic positions

and having different geometry and connectivity to the framework, which may perform differently in catalysis.

A synthetic method enabling control over sub-nm characteristics of active sites in zeolites would facilitate an evaluation of each individual characteristic of acid centers in a zeolite on its catalytic performance, contributing to replacing the current “trial-and-error” research strategy for rational engineering of targeted catalytic functions.

The author thanks to prof. J. Čejka for the guidance and support in various phases of her scientific life and for valuable discussions and advice during the preparation of the Czech version of this manuscript. This work was supported by the Ministry of Education, Youth and Sports of the Czech Republic through the ERC_CZ project LL 2104.

The list of abbreviations

BAS	Brønsted acid sites
D4R	double-four-ring
IR spectroscopy	Infra-red spectroscopy
LAS	Lewis acid sites
MAS NMR	magic-angle spinning nuclear magnetic resonance
MPV reduction	Meerwein-Ponndorf-Verley reduction
S4R	single-four-ring
SC-IZA	Structure Commission of the International Zeolite Association
TEM	transmission electron microscopy
TOF	turnover frequency
XRD	X-ray diffraction

REFERENCES

1. Baerlocher C. and 20 co-authors, in the book: *Atlas of Zeolite Framework Types* (Baerlocher C., McCusker L. B., Olson D. H., ed.), p. 1. Elsevier Science B. V., Amsterdam 2007.
2. <https://chembam.com/online-resources/gcse-resources/cages/>, downloaded February 25, 2023.
3. Shamzhy M., Opanasenko M., Concepción P., Martínez A.: *Chem. Soc. Rev.* **48**, 1095 (2019).
4. Clatworthy E. B., Konnov S. V., Dubray F., Nesterenko N., Gilson J.-P., Mintova S.: *Angew. Chem., Int. Ed.* **59**, 19414 (2020).
5. Primo A., Garcia H.: *Chem. Soc. Rev.* **43**, 7548 (2014).
6. Hanefeld U., Lefferts L.: *Catalysis: An Integrated Textbook for Students*. Wiley, 2018.
7. https://europe.iza-structure.org/IZA-SC/ftc_table.php, downloaded February 25, 2023.
8. Gottardi G., Galli E., in the book: *Natural Zeolites* (Gottardi G., Galli E., ed.), p. 1. Springer, Berlin 1985.
9. Cundy C. S., Cox P. A.: *Microporous Mesoporous Mater.* **82**, 1 (2005).
10. Suib S. L., Přech J., Szaniawska E., Čejka J.: *Chem. Rev. (Washington, DC, U. S.)* **123**, 877 (2023).
11. <https://www.earthmagazine.org/article/mineral-resource-month-zeolites/>, downloaded February 25, 2023.
12. Moliner M., Rey F., Corma A.: *Angew. Chem., Int. Ed.* **52**, 13880 (2013).
13. Li S., Tuan V. A., Falconer J. L., Noble R. D.: *Microporous Mesoporous Mater.* **58**, 137 (2003).
14. Wenten I. G., Dharmawijaya P. T., Aryanti P. T. P., Mukti R. R., Khoiruddin: *RSC Adv.* **7**, 29520 (2017).
15. O'Keefe M., Yaghi O. M.: *Chem. Eur. J.* **5**, 2796 (1999).
16. Opanasenko M., Shamzhy M., Wang Y., Yan W., Nachtigall P., Čejka J.: *Angew. Chem., Int. Ed.* **59**, 19380 (2020).
17. Paillaud J. L., Harbuzaru B., Patarin J., Bats N.: *Science* **304**, 990 (2004).
18. Corma A., Diaz-Cabanas M. J., Rey F., Nicolououlas S., Boulahya K.: *Chem. Commun. (Cambridge, U. K.)* 1356 (2004).
19. Corma A., Rey F., Valencia S., Jorda J. L., Rius J.: *Nat. Mater.* **2**, 493 (2003).
20. Lorgouilloux Y., Dodin M., Mugnaioli E., Marichal C., Caullet P., Bats N., Kolb U., Paillaud J. L.: *RSC Adv.* **4**, 19440 (2014).
21. Kang J. H., Xie D., Zones S. I., Smeets S., McCusker L. B., Davis M. E.: *Chem. Mater.* **28**, 6250 (2016).
22. Jiang J. X., Yu J. H., Corma A.: *Angew. Chem., Int. Ed.* **49**, 3120 (2010).
23. Roth W. J., Shvets O. V., Shamzhy M., Chlubná P., Kubů M., Nachtigall P., Čejka J.: *J. Am. Chem. Soc.* **133**, 6130 (2011).
24. Shamzhy M., Opanasenko M., Tian Y., Konysheva K., Shvets O., Morris R. E., Čejka J.: *Chem. Mater.* **26**, 5789 (2014).
25. Shamzhy M., Mazur M., Opanasenko M., Roth W. J., Čejka J.: *Dalton Trans.* **43**, 10548 (2014).
26. Eliášová P., Opanasenko M., Wheatley P. S., Shamzhy M., Mazur M., Nachtigall P., Roth W. J., Morris R. E., Čejka J.: *Chem. Soc. Rev.* **44**, 7177 (2015).
27. Kasneryk V., Shamzhy M., Zhou J., Yue Q., Mazur M., Mayoral A., Luo Z., Morris R. E., Čejka J., Opanasenko M.: *Nat. Commun.* **10**, 5129 (2019).
28. Firth D. S. a 11 co-authors: *Chem. Mater.* **29**, 5605 (2017).
29. Kasneryk V., Shamzhy M., Opanasenko M., Wheatley P. S., Morris S. A., Russell S. E., Mayoral A., Trachta M., Čejka J., Morris R. E.: *Angew. Chem., Int. Ed.* **56**, 4324 (2017).
30. Kasneryk V., Shamzhy M., Opanasenko M., Wheatley P. S., Morris R. E., Čejka J.: *Dalton Trans.* **47**, 3084 (2018).
31. Shamzhy M. V., Opanasenko M. V., Ramos F. S. d. O., Brabec L., Horáček M., Navarro-Rojas M., Morris R. E., Pastore H. d. O., Čejka J.: *Catal. Sci. Technol.* **5**, 2973 (2015).
32. Shamzhy M. V., Eliášová P., Vitvarová D., Opanasenko M. V., Firth D. S., Morris R. E.: *Chem. Eur. J.* **22**, 17377 (2016).
33. Kasneryk V., Opanasenko M., Shamzhy M., Musilová Z., Avadhut Y. S., Hartmann M., Čejka J.: *J. Mater. Chem. A* **5**, 22576 (2017).
34. Shvets O. V., Shamzhy M. V., Yaremov P. S., Musilová Z., Procházková D., Čejka J.: *Chem. Mater.* **23**, 2573 (2011).
35. Shamzhy M. V., Shvets O. V., Opanasenko M. V., Yaremov P. S., Sarkisyan L. G., Chlubná P., Zukal A., Marthala V. R., Hartmann M., Čejka J.: *J. Mater. Chem.* **22**, 15793 (2012).
36. Žilková N., Shamzhy M., Shvets O., Čejka J.: *Catal. Today* **204**, 22 (2013).
37. Shamzhy M. V., Ochoa-Hernández C., Kasneryk V. I., Opanasenko M. V., Mazur M.: *Catal. Today* **277**, 37 (2016).
38. Shamzhy M. V., Shvets O. V., Opanasenko M. V., Kurfířtová L., Kubička D., Čejka J.: *ChemCatChem* **5**, 1891 (2013).
39. Shamzhy M., Ramos F. S. d. O.: *Catal. Today* **243**, 76 (2015).
40. Sartori G., Maggi R.: *Chem. Rev. (Washington, DC, U. S.)* **106**, 1077 (2006).
41. Heard C. J., Grajciar L., Uhlík F., Shamzhy M., Opanasenko M., Čejka J., Nachtigall P.: *Adv. Mater. (Weinheim, Ger.)* **32**, 2003264 (2020).
42. Zhang J., Veselý O., Tošner Z., Mazur M., Opanasenko M., Čejka J., Shamzhy M.: *Chem. Mater.* **33**, 1228 (2021).
43. Zhou Y., Kadam S. A., Shamzhy M., Čejka J., Opanasenko M.: *ACS Catal.* **9**, 5136 (2019).

44. Abdi S., Kubů M., Li A., Kalíková K., Shamzhy M.: *Catal. Today* 390-391, 326 (2022).
45. Zhang J., Yue Q., Mazur M., Opanasenko M., Shamzhy M. V., Čejka J.: *ACS Sust. Chem. Eng.* 8, 8235 (2020).
46. Bordiga S., Lamberti C., Bonino F., Travert A., Thibault-Starzyk F.: *Chem. Soc. Rev.* 44, 7262 (2015).
47. Shamzhy M., Přeč J., Zhang J., Ruaux V., El-Siblani H., Mintova S.: *Catal. Today* 345, 80 (2020).
48. Shamzhy M., Gil B., Opanasenko M., Roth W. J., Čejka J.: *ACS Catal.* 11, 2366 (2021).
49. Podolean I., Zhang J., Shamzhy M., Pârvulescu V. I., Čejka J.: *Catal. Sci. Technol.* 10, 8254 (2020).
50. Zhang Y., Li A., Kubů M., Shamzhy M., Čejka J.: *Catal. Today* 390-391, 295 (2022).